A Single Amino Acid Substitution Changes Ribonuclease 4 from a Uridine-Specific to a Cytidine-Specific Enzyme[†]

Jan Hofsteenge,* Carina Moldow, Anna M. Vicentini, Ottilie Zelenko,[‡] Zsophie Jarai-Kote, and Ulf Neumann[§]

Friedrich Miescher-Institut, P.O. Box 2543, CH-4002 Basel, Switzerland

Received February 18, 1998; Revised Manuscript Received April 10, 1998

ABSTRACT: The structural features underlying the strong uridine specificity of ribonuclease 4 (RNase 4) are largely unknown. It has been hypothesized that the negatively charged α-carboxylate is close to the pyrimidine binding pocket, due to a unique C-terminal deletion. This would suppress the cleavage of cytidine-containing substrates [Zhou, H.-M., and Strydom, D. J. (1993) *Eur. J. Biochem. 217*, 401−410]. Replacement of the α-carboxylate by an α-carboxamide in a fragment complementation system decreased both $(k_{cat}/K_m)_{CpA}$ and $(k_{cat}/K_m)_{UpA}$, thus refuting the hypothesis. However, model building showed that the deletion allowed the side chain of Arg-101 to reach the pyrimidine binding pocket. From the 386-fold reduction in $(k_{cat}/K_m)_{UpA}$ in RNase 4;R101N, it is concluded that this residue functions in uridine binding, analogous to Ser-123 in RNase A. In addition, it may have an effect on Asp-80. The 2-fold increase in $(k_{cat}/K_m)_{CpA}$ in the mutant R101N and the close proximity of the side chains of Arg-101 and Asp-80 suggested that the latter could be involved in suppressing CpA catalysis. The substrate specificity of RNase 4;D80A was completely reversed: $(k_{cat}/K_m)_{UpA}$ decreased 159-fold, whereas $(k_{cat}/K_m)_{CpA}$ increased 233-fold. The effect on CpA was unexpected, because the corresponding residue in bovine pancreatic RNase A (Asp-83) hardly affects cytidine-containing substrates. Furthermore, the residue is conserved in nearly all sequences of mammalian RNase 1. Thus, an evolutionary highly conserved residue does not necessarily function in the same way in homologous enzymes. A model, which proposes that the structure of RNase 4 has been optimized to permanently fix the position of Asp-80 and impede its movement away from the pyrimidine binding pocket, is presented.

Mammalian ribonucleases (RNases)[1] that are homologous to bovine pancreatic RNase A [called pancreatic-type RNases (*2*, *3*)] form a superfamily that can be divided into five subfamilies on the basis of sequence homology (*1*). All enzymes cleave RNA exclusively after pyrimidines. The mechanism of cleavage of the phosphodiester bond has been examined in detail in bovine pancreatic RNase A (*4*, *5*). Because the essential catalytic residues have been completely conserved, the catalytic mechanism appears to be the same for all RNases belonging to this superfamily. The pyrimidine specificity of the enzymes results from the binding of the base in a narrow pocket on the surface of the enzyme, the so-called B1 subsite. In RNase A this binding site is formed by His-12, Val-43, Asn-44, Thr-45, and Phe-120 (*4*). In particular, Thr-45 plays an important role (*6*); its =NH donates a hydrogen bond to O2 of either pyrimidine base, whereas its $^{\gamma}$OH acts as a hydrogen bond acceptor in the case of uridine but as a donor in the case of cytidine. X-ray and/or site-directed mutagenesis studies have shown that this residue, which has been conserved in all RNases sequenced to date, is also involved in pyrimidine binding in RNases belonging to three other subfamilies, i.e., RNase 2 [also called eosinophil-derived neurotoxin (*7*)], angiogenin (*8*, *9*), and RNase 4[2] (*10*). Furthermore, Phe-120 in RNase A is in van der Waals contact with the pyrimidine base. Similar interactions are likely to take place in RNase 2 and angiogenin, where the Phe has been replaced by a Leu residue, and in RNase 4, which also contains a Phe at this position. A summary of the function of the B1 subsite residues has been given in Table 1, whereas the sequences of RNase 4 and RNase A have been compared in Figure 1.

Despite the structural conservation of these important binding residues, the discrimination between cytidine and uridine by these four RNases differs greatly. Whereas RNase A cleaves the dinucleotides CpA and UpA about equally well, RNase 2 and angiogenin prefer CpA over UpA by a factor of 2 and 11, respectively (*11*, *12*). Furthermore, RNase 4 is a strongly uridine-preferring enzyme, cleaving UpA 380-fold faster than CpA (*13*, *14*). These results suggest that

[†] C.M. was supported by grants from the Erasmus program and Otto Hønsted fund.

* To whom correspondence should be addressed: telephone, 061 697 47 22; fax, 061 697 39 76; e-mail, hofsteen@fmi.ch.

[‡] Present address: Department of Molecular and Cell Biology, University of California, Berkeley, CA.

[§] Present address: Novartis AG, CH-4002 Basel, Switzerland.

[1] Abbreviations: CpA, cytidylyl-(3′,5′)-adenosine; CPA, carboxypeptidase A; CPB, carboxypeptidase B; CPY, carboxypeptidase Y; CysCM, (carboxymethyl)cysteine; LC-ESIMS, liquid chromatography interfaced with electrospray ionization mass spectrometry; MALDI-TOF-MS, matrix-assisted laser desorption/ionization time-of-flight mass spectroscopy; Mes, 2-morpholinoethanesulfonic acid; RNase, ribonuclease; TFA, trifluoroacetic acid; UpcA, UpA with the 5′-oxygen of the ribose replaced by a methylene group; UpA, uridylyl-(3′,5′)-adenosine.

[2] This RNase has previously been called RNase PL3. The nomenclature of Zhou and Strydom (*1*) is preferred and used here.

S0006-2960(98)00383-3 CCC: $15.00
Published on Web 06/05/1998

Table 1: B1 Subsite and Auxiliary Residues in RNase A and RNase 4

RNase A	RNase 4	function in RNase A
B1 subsite residues that contact the base		
Val-43	Phe-42	van der Waals contacts with the pyrimidine
Thr-45	Thr-44	hydrogen bonds to pyrimidine
Phe-120	Phe-117	van der Waals contacts with the base
auxiliary residues[a]		
Asp-83	Asp-80	hydrogen bonds to Thr-45 $^{\gamma}$O
Ser-123	deleted	binds to uracil O4 via water molecules

[a] Residues that do not contact the pyrimidine base but interact with residues (or water molecules) that do.

```
          1                  10                  20                  30
pRNase 4 <Q D R M Y Q R F L R Q H V D P D . A T G G N D A Y C N L M M Q
RNase A   K E T A A A K F E R Q H M D S S T S A A S S S N Y C N Q M M K
          1                  10                  20                  30
                               # *

                             40                  50                  60
pRNase 4  R R K M T S H Y C K R F N T F I H E D I W N I R S I C S T S
RNase A   S R N L T K D R C K P V N T F V H E S L A D V Q A V C S Q K
                           40                  50                  60
                             *   # # #

                             70                  80                  90
pRNase 4  N I Q C K N G Q M N C H E . . G V V K V T D C R E T G S S R A P
RNase A   N V A C K N G Q T N C Y Q S Y S T M S I T D C R E T G S S K Y P
                           70                  80                  90
                  #

                            100                 110                 119
pRNase 4  N C R Y R A M A S T R R V V I A C E G N P E V P V H F D K
RNase A   N C A Y K T T Q A N K H I I V A C E G N P Y V P V H F D A S V
                  100                 110                 120     124
                                        #                 * # *   #
```

FIGURE 1: Comparison of the primary structures of porcine RNase 4 and bovine pancreatic RNase A. The numbering for pRNase 4 and RNase A is shown above and below the sequences, respectively. Catalytic residues have been indicated with *, whereas residues that are involved in substrate binding have been marked with #. Asp-80 and Arg-101 in pRNase 4 have been underlined. <Q denotes pyroglutamic acid.

the pyrimidine binding properties are determined by structural features that are outside of the B1 subsite and are different in the four enzymes (*10*).

Comparison of the values of k_{cat}/K_m for the cleavage of UpA and CpA by RNase 4 (2.5×10^5 and 6.6×10^2 M^{-1} s^{-1}) and RNase A (3.5×10^6 and 4.6×10^6 M^{-1} s^{-1}) reveals that the uridine specificity of the former results from a suppression of the activity with cytidine-containing substrates. Two residues that are involved in this suppression are Phe-42 and Thr-44, both part of the B1 subsite, since mutation into Val and Ala caused an increase in activity with CpA and poly(C) (*10*). The double mutant F42V/T44A cleaved CpA 10-fold better than UpA. However, the absolute value of k_{cat}/K_m of this mutant with CpA (1.3×10^4 M^{-1} s^{-1}) is still 19-fold lower than that of the wild-type enzyme with UpA. This must mean that still other parts of the RNase 4 structure are suppressing the activity with CpA. In RNase A auxiliary residues have been identified that do not directly form part of the B1 subsite but influence its properties. Asp-83 exerts its effect by hydrogen bonding to $^{\gamma}$O of Thr-45 (*15*) and Ser-123 by participating in a hydrogen-bonding network with water molecules that interact with the base in the B1 subsite (*16*).

A feature that distinguishes RNase 4 from all other RNases of the superfamily is its shorter C-terminus. Compared to RNase A this could have two consequences: (i) in RNase 4 the negatively charged C-terminal α-carboxylate is in close proximity to the pyrimidine-binding pocket (*1*); (ii) Ser-123 is missing, but the shorter C-terminus provides room for a residue from another part of the molecule to take its position (*14*). Alternatively, the role of the other auxiliary residue, Asp-80, differs between RNase 4 and the cytidine-preferring RNases.

Here these hypotheses are tested. The effect of the negatively charged α-carboxylate of RNase 4 on its substrate specificity has been examined using a fragment complementation system, consisting of residues 1−115 of RNase 4 and either the natural or the C-terminally amidated peptide 111−119. Model building strongly suggested that, mainly because of the shortened C-terminus, Arg-101 (Lys-104 in RNase A) could approximately take the position of Ser-123 in RNase A. Its importance, and that of Asp-80, for substrate cleavage has been examined by kinetic analysis of the site-directed mutants.

MATERIALS AND METHODS

Materials. Bovine pancreatic RNase A, carboxypeptidases A, B, and Y, and pepsin were from Boehringer Mannheim, FRG. Buffer substances were obtained from Fluka, Switzerland. UpA and CpA were obtained from Dr. A. Okrusek, Warsaw, Poland. Recombinant porcine RNase 4 was prepared and purified as described (*14*).

Protein Chemistry. Reversed-phase HPLC was done using Vydac C_4 or C_{18} columns and a trifluoroacetic acid solvent system (*17*). A flow rate of 0.2 mL/min and columns with 2.1 mm diameter were used for analytical purposes, whereas for preparative runs 4.6 and 10 mm columns at a flow rate of 0.5 and 2 mL/min were used.

Fast protein liquid chromatography was done on a Pharmacia FPLC system and a Mono S column using buffer A,

15 mM phosphate pH 6.0, and buffer B, 500 mM phosphate, pH 6.0. Proteins were detected at 280 nm.

Tryptic peptide mapping was done as described (*14*). Amino acid analysis was done using the dabsyl chloride method (*18*). The incorporation of the C-terminal lysinamide in one of the synthetic peptides was demonstrated using a modification of this method (*19*).

Edman degradation was performed with an Applied Biosystems 477A sequencer. Peptide and protein masses were determined on a Canyon Creek LDI 1700 MALDI-TOF-MS or on an API 300 triple quadrupole mass spectrometer. Peptide synthesis was done at the peptide synthesis facility at the FMI using the solid-phase/fluoren-9-ylmethoxycarbonyl (Fmoc) strategy. All peptides were purified by preparative reversed-phase HPLC, and the purity was analyzed by analytical HPLC and amino acid analysis.

Preparation of Des(116−119)-RNase 4. Recombinant porcine RNase 4 (165 μg) was dried in a speedvac and dissolved in 330 μL of 50 mM NH_4HCO_3, pH 8.3, containing 6 M urea. CPB (22 μL, 0.5 mg/mL) was added, and the mixture was incubated at 37 °C for 45 min, which yielded des(119)-RNase 4. Des(119)-RNase 4 (100 μL from the previous step) was mixed with urea−acetate buffer, pH 4.8 (260 mg of urea plus 518 μL of 1 M acetic acid plus 230 μL of water). CPY (8.1 μL, 15.7 μM) was added, and the reaction was stopped after 3 min by the addition of 150 μL of 1% TFA. The digestion mixture containing des(118−119)-RNase 4 was fractionated by HPLC. Des(118−119)-RNase 4 was digested with CPA to yield des(116−119)-RNase 4, as described for RNase A (1−118) (*20*), and purified by FPLC.

Preparation of RNase A (1−122). RNase A (1−122) was prepared by first unfolding the enzyme in 10 M urea and subsequent dilution of the denatured enzyme into Tris buffer containing CPY. After dilution, refolding of the enzyme and digestion by CPY occurred simultaneously. The cleaved, refolded enzyme is protected against further digestion by CPY (*21*). CPY was dialyzed against water overnight and concentrated to 90 μM in a Centricon-30 microconcentrator (Amicon). RNase A (5 mg) was dissolved in 10 M urea in 0.1 M sodium phosphate, pH 6.3, to a final concentration of 100 mg/mL, and the mixture was incubated at 37 °C for 1 h. The unfolded RNase (50 μL) was diluted into a mixture of 300 μL of Tris−acetate buffer, pH 8.3, 75 μL of CPY was added, and the mixture was incubated for 4 min. The mixture was loaded onto a Mono S column, and proteins were eluted with a gradient from 0 to 200 mM NaCl in 20 mM Hepes−NaOH, pH 8.0, over 60 min at a flow rate of 1 mL/min. The peak eluting before native RNase A was collected, and the proteins were purified by reversed-phase HPLC on a Vydac C_4 column with a linear gradient from 14% to 42% acetonitrile in 45 min. RNase A (1−122) (260 μg) was found to be pure by SDS−PAGE, analytical HPLC, and tryptic peptide mapping.

Site-Directed Mutagenesis and Expression of Recombinant RNase 4. Mutagenesis was performed using the cDNA coding for RNase 4 described previously (*14*). Mutations were introduced by overlap extension using PCR (*22*) and verified by dideoxy sequencing (*23*) of both strands. The mutant RNase 4's were purified as described (*14*). Their purity was assessed by SDS−PAGE and reversed-phase LC-ESIMS.

Kinetic Measurements. Kinetic analysis of the transesterification reaction with the dinucleotides UpA and CpA was performed at 25 °C in 50 mM Mes−NaOH, pH 6.0, containing 125 mM NaCl, 1 mM EDTA, 0.1% poly(ethylene glycol), and 0.2 mg/mL bovine serum albumin (*24*). The decrease in absorbance at 294 nm was measured with a Hewlett-Packard 8452A spectrophotometer. The dissociation constant, K_d, of the noncovalent peptide−RNase complexes was determined using UpA as a substrate. The concentrations of both the truncated RNase and peptide were determined by amino acid analysis. Peptide (P) and truncated RNase (E) were mixed in buffer and incubated for 10 min at 25 °C, and the reaction was started by addition of UpA (final concentration 66 μM). The pseudo-first-order progress curve of substrate disappearance was followed for at least 5 half-lives. Under conditions where $[P_0] \gg [E_0]$ and $[S_0] \ll K_m$, the pseudo-first-order rate constant can be described by

$$k_{obs} = (k_{cat}/K_m)[E_0][P_0]/(K_d + [P_0]) \quad (1)$$

where $[E_0]$ and $[P_0]$ are the starting concentrations of truncated RNase and peptide, respectively, and K_d is the dissociation constant of the complex. The rate constant, k_{obs}, obtained at seven concentrations of peptide was fitted to eq 1, which yielded estimates for the value of K_d as well as the specificity constant, k_{cat}/K_m, of the protein−peptide complex. To determine the values of k_{cat}/K_m for the substrate CpA, the peptide concentration in the assay was adjusted to $10 \times K_d$, and the progress curve was recorded using 50 μM CpA.

The enzymatic activity of mutant RNase 4's with the substrates UpA and CpA was determined under pseudo-first-order conditions as described above. The pseudo-first-order rate constant, k_{obs}, was obtained at four different enzyme concentrations, from which the value of k_{cat}/K_m was obtained by linear regression. At least three independent experiments were performed.

Model Building. A model of the pyrimidine binding site of RNase 4 was built manually, based on the coordinates of 6rsa.pdb, using the program Insight II (BIOSYM/Molecular Simulations, San Diego, CA). Residues 123−124 of RNase A were deleted, and Val-43, Ile-81, and Lys-104 were replaced by the corresponding residues of RNase 4, i.e., Phe-42, Val-78, and Arg-101. The conformation of the main chain was not altered, whereas that of the side chains of Arg-101 and Phe-42 was adjusted. No energy minimization was performed, but overlap of van der Waals radii was verified using the "bump-check" option of the Insight II program. In addition, the entire molecule was submitted to SWISS-MODEL (*25*), which used the coordinates of free RNase (7rsa.pdb).

RESULTS

Fragment Complementation System of RNase 4. It has been proposed that the close proximity of the α-carboxylate to the pyrimidine binding pocket of RNase 4 has an effect on catalysis (*1*). Previous attempts to test this hypothesis by replacing Lys-119 with the C-terminal sequence of bovine pancreatic RNase A (-Ala-Ser-Val) by mutagenesis failed, due to the recovery of minute amounts of inactive RNase 4 mutant (*14*). Therefore, a fragment complementation system consisting of des(116−119)-RNase 4 and C-terminal peptides was established as follows.

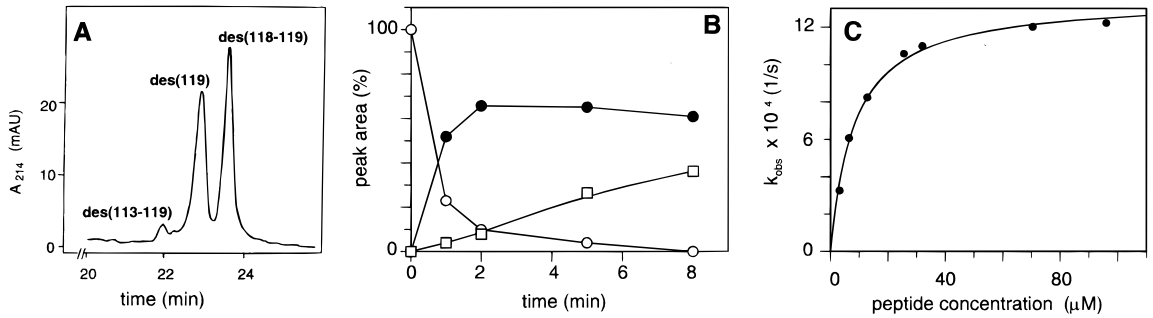

FIGURE 2: Digestion of des(119)-RNase 4 with carboxypeptidase Y. (A) Reversed-phase HPLC of the reaction products. Des(119)-RNase 4 was digested for 1 min with CPY at pH 4.8. The mixture was chromatographed on a C_4 column equilibrated in 0.1% TFA. Elution was achieved with a linear gradient of CH_3CN. The protein in each peak was identified by peptide mapping and analysis of the C-terminal peptide. (B) Time course of CPY digestion. Samples were taken at the indicated times, acidified, and analyzed as described in "A". The peak area for each molecular species was determined by integration: (○) des(119)-RNase 4; (●) des(118−119)-RNase 4; (□) des(113−119)-RNase 4. (C) Complex formation between des(116−119)-RNase 4 and the C-terminal peptides was monitored by measuring the pseudo-first-order rate constant for cleavage of UpA (66 μM). The results obtained with peptide **1** (PYVPVHFDK) and 6.2 nM des(116−119)-RNase 4 are shown. The solid line shows the best fit of the data to eq 1 (Materials and Methods), yielding values for the dissociation constant of the protein−peptide complex, K_d, and its catalytic efficiency k_{cat}/K_m (summarized in Table 2).

Table 2: Kinetic Parameters of Derivatives of Des(116−119)-RNase 4/Peptide Complexes and of Truncated RNase A[a]

	k_{cat}/K_m (M^{-1} s^{-1})		
	UpA	CpA	K_d (μM)
RNase 4[b]	2.5×10^5	6.6×10^2	
des(116−119)-RNase 4			
+PYVPVHFDK (**1**)	$(2.10 \pm 0.03) \times 10^5$	$(5.67 \pm 0.02) \times 10^2$	7.0 ± 0.5
+PYVPVHFDK-NH_2 (**2**)	$(1.29 \pm 0.08) \times 10^4$	$(1.33 \pm 0.06) \times 10^2$	18.0 ± 3.2
+PYVPVHFDASV (**3**)	$(1.72 \pm 0.03) \times 10^4$	$(4.79 \pm 0.02) \times 10^2$	7.2 ± 0.6
RNase A[b]	3.5×10^6	4.6×10^6	
des(123−124)-RNase A	$(0.35 \pm 0.02) \times 10^6$	$(4.0 \pm 0.18) \times 10^6$	

[a] Kinetic parameters were determined in 50 mM Mes, $I = 0.150$, pH 6.0 at 25 °C as described in Materials and Methods. The values given are the weighted means, together with their standard errors, of duplicate experiments. [b] Data were taken from ref *14*.

Des(116−119)-RNase 4 was produced by a stepwise procedure using different carboxypeptidases. Incubation of RNase 4 with CPB in the presence of 6 M urea yielded des-(119)-RNase 4, as expected (C-terminal sequence -His^{116}-Phe-Asp^{118}-OH). Des(119)-RNase 4 was further digested with carboxypeptidase Y (CPY) to yield des(118−119)-RNase 4. This reaction was found to be the crucial step in the entire preparation and was investigated in more detail. CPY digestion as a function of pH in the range from 4.8 to 7.4 showed that at neutral pH values des(113−119)-RNase 4 was the only reaction product. On the other hand, at pH values below 5, a substantial amount of des(118−119)-RNase 4 accumulated as well (Figure 2A). Under slightly acidic conditions the relative cleavage rate of the Phe^{117}−Asp^{118} bond was increased, probably due to partial protonation of the carboxyl side chain, and protonation of His-116 slowed the cleavage of the His^{116}−Phe^{117} bond. The time course of the reaction at pH 4.8 was also determined (Figure 2B). It was found that after 2 min des(119)-RNase 4 was nearly completely converted into des(118−119)-RNase 4 but that at later time points the formation of des(113−119)-RNase 4 became significant. Des(118−119)-RNase 4 was isolated from a 2 min digest of des(119)-RNase 4 and was further digested with CPA to yield des(116−119)-RNase 4 (see Materials and Methods). The purified, inactive, protein was characterized by amino acid analysis and tryptic peptide mapping. A single peptide was obtained from the C-terminal region, which by Edman degradation yielded the sequence Arg-Val-Val-Ile-Ala-CysCm-Glu-Gly-Asn-Pro-Glu-Val-Pro-Val, corresponding to residues 102−115. Moreover, its molecular mass as determined by MALDI-TOF-MS was in agreement with the calculated value.

Complementation of Des(116−119)-RNase 4 by C-Terminal Peptides. Addition of increasing amounts of the C-terminal peptide PYVPVHFDK (**1**) to des(116−119)-RNase 4 increased RNase activity in a saturable manner (Figure 2C). Analysis of the data according to eq 1 (see Materials and Methods) yielded the value for k_{cat}/K_m and an estimate of the dissociation constant of the protein−peptide complex, K_d (Table 2). The catalytic efficiency of the complex with peptide **1** for the substrates UpA and CpA was nearly the same as that of native RNase 4 (Table 2).[3]

The system was used to study the influence of the negatively charged α-carboxylate on the catalytic properties of RNase 4. Des(116−119)-RNase 4 was complexed with the synthetic peptides shown in Table 2, resulting in structures similar to RNase 4 (**1**), to RNase 4 with an amidated C-terminus (**2**), and to RNase A (**3**). The catalytic properties were determined as shown in Figure 2C, and the values obtained for k_{cat}/K_m and K_d have been summarized in Table 2. Replacement of the negatively charged C-terminal α-carboxylate by a neutral carboxamide, as in peptide **2**, reduced the catalytic efficiency toward UpA 16-fold. Also, the complex with peptide **3** (PYVPVHFDASV) had a strongly decreased activity toward this substrate. Toward

[3] Peptide **1** contains Tyr at position 2 instead of Glu (as in RNase 4) to facilitate the determination of its concentration. The nearly complete recovery of enzymatic activity with des(116−119)-RNase 4 showed that this substitution did not influence the catalytic properties.

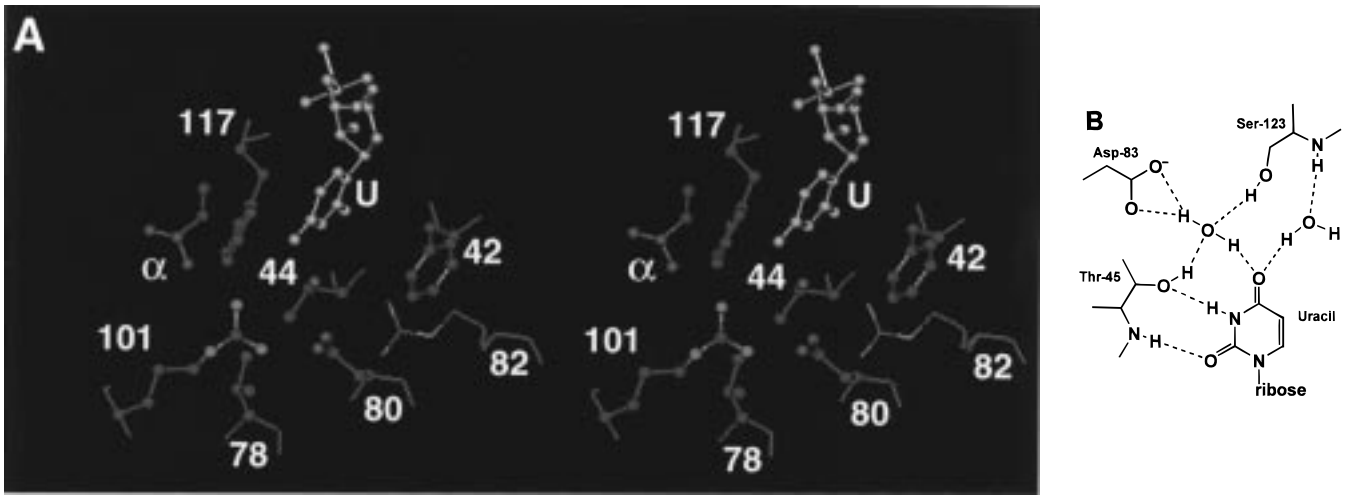

FIGURE 3: Pyrimidine-binding site in RNase 4 and RNase A. (A) Stereo diagram of the modeled pyrimidine binding site in RNase 4. The uridine vanadate is shown in magenta. The side chain of Arg-82 is in too close contact with Phe-42 but has been included to demonstrate the effect on the Asp-80−Arg-82 interaction (see Discussion). The α-carboxylate has been indicated with α. The coordinates for this model were taken from 6rsa.pdb (*26*). (B) Mode of binding of uracil in the B1 subsite of RNase A. This figure has been adapted from that in ref *16*.

CpA, however, the complex with the amidated peptide **2** had a 4-fold reduced k_{cat}/K_m (Table 2). In contrast, the complex formed with the (longer) C-terminal peptide of RNase A (**3**) was almost as active toward CpA as that with the native RNase 4 C-terminus.

These results demonstrated the importance of the α-carboxylate in RNase 4 for the cleavage of, in particular, UpA. It was therefore of interest to investigate whether a shortened C-terminus would generally cause uridine specificity in pancreatic-type RNases. Bovine pancreatic RNase A was shortened by two amino acids [des(123−124)-RNase A]. Removal of Ser-123 and Val-124 in this enzyme did not result in uridine specificity. Whereas k_{cat}/K_m for UpA decreased 10-fold, that for CpA dropped only 1.2-fold (Table 2).

Model of the Pyrimidine Binding Site of RNase 4. A model of the B1 subsite of RNase 4 was built using the coordinates of the RNase A−uridine vanadate complex [6rsa.pdb (*26*)]. In the initial model a large open space was present close to the B1 subsite, due to the deletion of the two C-terminal residues. Inspection of the model indicated that either the side chain of Lys-119 or that of Arg-101 (the C-terminal residue of β-strand 94−101) could point into the pyrimidine binding site (Figure 3A). In RNase A Ser-123 is important for binding uridine (Figure 3B, Table 1, and refs *16* and *27*) but not cytidine (*28*). To discern whether possibly Lys-119 or Arg-101 in RNase 4 takes over the role of Ser-123, site-directed mutants were prepared.

Isolation and Characterization of Mutants of RNase 4. All mutant proteins could be purified by the standard procedure described in Materials and Methods. The proteins were judged to be pure from analysis by SDS−PAGE and LC-ESIMS. Their molecular masses were in good agreement with the theoretical values (see footnote to Table 3).

The values for k_{cat}/K_m for the mutated RNase 4's with the substrates UpA and CpA have been summarized in Table 3. The K119A mutation had only a minor, improving, effect on the catalytic efficiency of both substrates. This is in agreement with the occurrence of Gly at position 119 in human RNase 4, which is functionally indistinguishable from the porcine enzyme (*13*). In contrast, mutation of Arg-101 caused a 385-fold decrease in $(k_{cat}/K_m)_{UpA}$ but a minor (1.9-fold) increase in $(k_{cat}/K_m)_{CpA}$. The same effect was observed for the mutant R101A, excluding the possibility that new alternative interactions of the Asn side chain were involved.

Table 3: Kinetic Parameters of Mutants of RNase 4[a]

	k_{cat}/K_m (M^{-1} s^{-1})	
	UpA	CpA
RNase 4[b]	2.5×10^5	6.6×10^2
RNase 4;R101N[c]	$(6.5 \pm 0.1) \times 10^2$	$(1.23 \pm 0.02) \times 10^3$
RNase 4;D80A[c]	$(1.57 \pm 0.09) \times 10^3$	$(1.54 \pm 0.02) \times 10^5$
RNase 4;K119A[c]	$(4.3 \pm 0.1) \times 10^5$	$(7.7 \pm 0.1) \times 10^2$

[a] Kinetic parameters were determined as described in Table 2. The values are the weighted means, together with their standard errors, of at least three independent experiments. [b] Data were taken from ref *14*. [c] Molecular masses of the mutant proteins: RNase 4;R101N, 13 783 Da (exp 13 786 Da); RNase 4;D80A, 13 765 Da (exp 13 767 Da); RNase 4;K119A, 13 753 Da (exp 13 753 Da).

The effect of the R101N mutation, together with the possible close proximity (Figure 3A) of the side chain of Arg-101 to that of Asp-80, the residue corresponding to Asp-83 in RNase A, suggested that the acidic residue could be involved in suppressing CpA catalysis. The effect of mutating Asp-80 was dramatic. The 159-fold decrease in catalytic efficiency with UpA and the concomitant 233-fold increase in the cleavage of CpA (Table 3) resulted in a cytidine-preferring RNase 4. The value of $(k_{cat}/K_m)_{CpA}$ of the mutant enzyme was nearly the same (61%) as that of $(k_{cat}/K_m)_{UpA}$ of the wild-type enzyme. The ratios of the specificity constants for UpA and CpA with the various RNase 4's have been summarized in Figure 4.

DISCUSSION

The clear-cut specificity of RNase 4 for uridine makes it an attractive object for the study of substrate specificity in the RNase A superfamily. Until now most of these kinds of studies have been performed with bovine RNase A, an RNase that cleaves equally well after cytidine and uridine (*6*, *15*), and angiogenin, a cytidine-preferring RNase (*9*). A

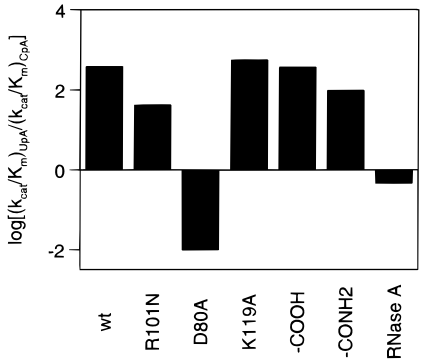

FIGURE 4: Substrate specificity of various RNase 4's. Note that the logarithm of the ratio of the specificity constants has been plotted. Values larger than 0 correspond to uridine-preferring RNases and those lower than 0 to cytidine-preferring ones.

comparison of the B1 subsite and auxiliary residues in RNase A with the sequence of RNase 4 reveals two major differences: The Val → Phe substitution at position 42 and the shortening of the C-terminus, which deletes Ser-123 (Table 1). The function of Phe-42 has previously been examined. Its mutation to Val improved the rate of cleavage of CpA much more than that of UpA, suggesting that it plays some role in suppressing activity with cytidine substrates (*10*) (see also below).

Here the role of the shortened C-terminus of RNase 4 has been analyzed. A brief overview of this part of the RNase A molecule is useful. The function of residues in the C-terminus of RNase A in determining substrate specificity has been examined kinetically (*28*) and by X-ray crystallography (*16*, *29*, *30*). The $^{\gamma}$OH of Ser-123 is thought to be important for binding to uridine but not to cytidine. The results obtained in this paper with des(123−124)-RNase A are in agreement with these studies. Deletion of Ser-123 and Val-124 resulted in a larger decrease in k_{cat}/K_m for UpA (10-fold) than for CpA (1.2-fold; Table 2). Gilliland et al. (*16*) have found that both ═NH and $^{\gamma}$OH of Ser-123 interact with uridine O4 through two conserved water molecules (Figure 3B). Although they proposed a similar network for the binding of cytidine, the much smaller effect of removal of Ser-123 on catalysis of cytidine substrates (Table 2) indicates that in this case the network is not as important.

For RNase 4 Zhou and Strydom (*1*) proposed that the shortened C-terminus causes a low activity with cytidine-containing substrates through an interaction between the free α-carboxylate and the cytidine amino function, which would prevent productive binding. The results shown in Table 2 contradict this hypothesis. The presence of the free α-carboxylate has a positive influence on the cleavage of CpA, as concluded from the 4-fold reduction of k_{cat}/K_m upon replacement by the neutral carboxamide. The $(k_{cat}/K_m)_{UpA}$ decreased 16-fold, showing that in the case of UpA this positive effect is stronger. The magnitude of this differential effect is, however, too small to explain the strong uridine-preferring specificity of RNase 4 (Figure 4). Also the results obtained with des(123−124)-RNase A show that a shorter C-terminus by itself does not confer uridine specificity onto an RNase (Table 2).

Vicentini et al. (*14*) have hypothesized that the shorter C-terminus allows other residues in RNase 4 to replace the function of Ser-123 in RNase A in the binding of uridine in the B1 subsite. The model in Figure 3A and the mutagenesis experiments (Table 3), in particular the 385-fold reduction in $(k_{cat}/K_m)_{UpA}$ upon mutation into Asn, strongly favor the notion that the side chain of Arg-101 fulfills this role. Its CZ atom can approximately occupy the position of $^{\gamma}$O of Ser-123 in RNase A, whereas its NH1 and NH2 groups could be close enough to the α-carboxylate and OD1 of Asp-80 to form hydrogen bonds. In the present model the distance between the guanidinium function and O4 of uridine is too big for a direct hydrogen bond. A plausible explanation for the reduction in $(k_{cat}/K_m)_{UpA}$ is that Arg-101 participates in a water network, like Ser-123 in RNase A (Figure 3B). Furthermore, Arg-101 may help in fixing the side chain of Asp-80 (see below). The slightly (1.9-fold) increased activity of RNase 4;R101N with CpA is insufficient to explain RNase 4's substrate specificity (Figure 4). An observation that strengthens the overall model is the substitution of Ile-81 in RNase A by the smaller Val-78 in RNase 4. A larger side chain at this position would sterically hinder access of the Arg-101 side chain to the B1 subsite. The aliphatic part of Arg-101 can nicely contact CG1 and CG2 of Val-78.

Because neither of the two major differences in the B1 subsite of RNase 4 (Table 1) could satisfactory explain the suppression of the cleavage of CpA, the possibility that Asp-80 is involved was examined. The results in Table 3 and Figure 4 clearly show that the D80A mutation caused a complete reversal of the specificity of RNase 4. It is concluded that this residue is essential for catalysis with UpA but that it suppresses at the same time that with CpA. The latter is a somewhat surprising finding, because the corresponding residue in RNase A, Asp-83, hardly has any influence on the rate of cleavage of poly(C), although it enhances that of poly(U) (*15*). The effect on poly(U) catalysis has been explained by the participation of Asp-83 in hydrogen bonding to Thr-45 $^{\gamma}$O, which would improve its capability to accept a hydrogen bond from uridine N3 (*15*). In nearly all other mammalian RNase 1's sequenced to date, this aspartate is present as well (*2*, *3*). These observations lead to the interesting concept that although the structure of Asp-80 is evolutionarily highly conserved between RNases 1 and 4, its exact function may have changed due to interactions with its environment. A similar, and probably functionally related, phenomenon has been observed for Thr-44 in RNase 4. Also, this residue is conserved in all pancreatic-type RNases, but its function differs in members of different subfamilies (*10*). Its site-directed replacement by Ala in RNase A decreases the efficiency of cleavage of uridine- and cytidine-containing substrates to approximately the same extent (*6*). In angiogenin the mutation reduces $(k_{cat}/K_m)_{CpA}$ 9-fold more than $(k_{cat}/K_m)_{UpA}$ (*9*), whereas in RNase 4 it increases $(k_{cat}/K_m)_{CpA}$ 5-fold but decreases $(k_{cat}/K_m)_{UpA}$ 300-fold (*10*, *14*).

The results presented here and in previous publications (*10*, *14*), are consistent with the following model to explain the substrate specificity of RNase 4: The B1 subsite is formed by Phe-42, Thr-44, and Phe-117, with the α-carboxylate and the side chains of Arg-101 and Asp-80 as auxiliary residues. Its structure appears to have been optimized to fix Asp-80 permanently in a position close to Thr-44 and the B1 subsite (Figure 3A). This would improve the hydrogen bond accepting properties of Thr-44, resulting in optimal binding of uridine (cf. ref *15*). It also causes

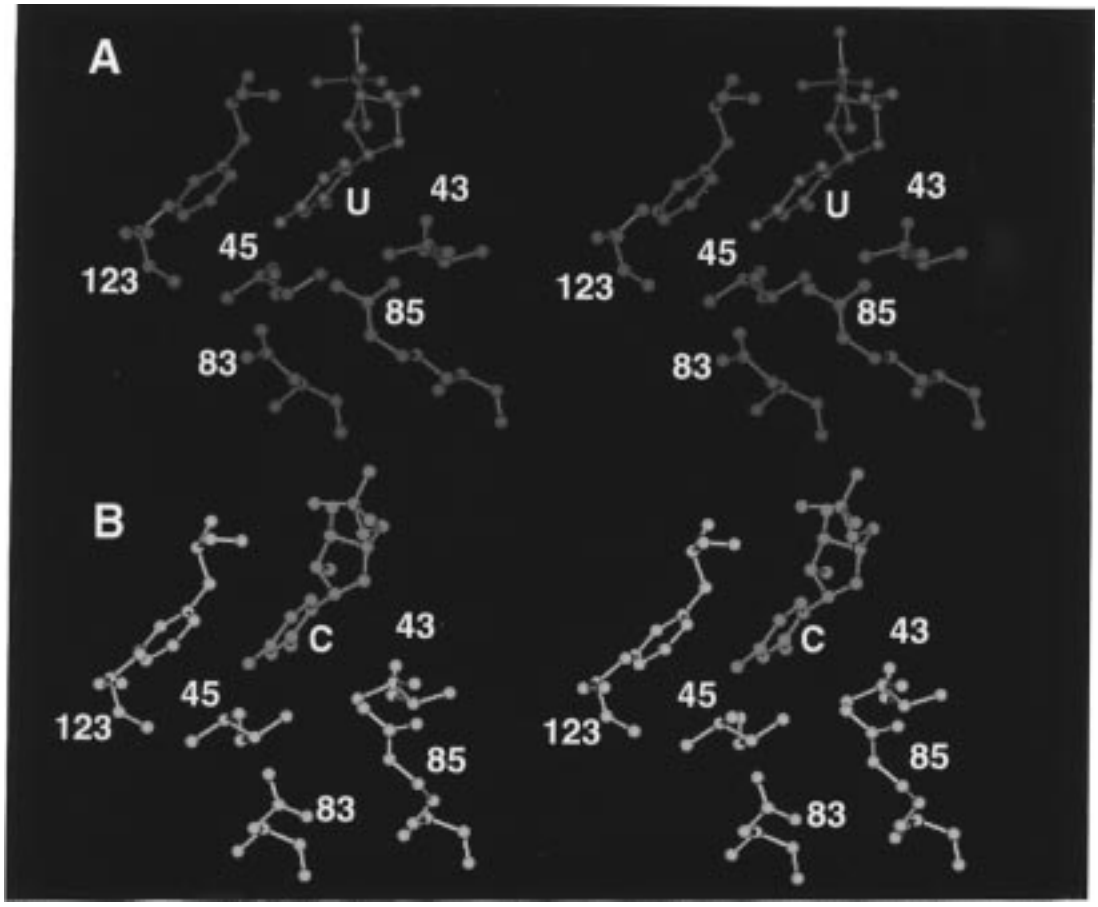

FIGURE 5: Position of Asp-83 in RNase A depends on the bound pyrimidine. (A) Pyrimidine binding pocket of RNase A with uridine vanadate (in red) bound. The coordinates for this diagram were taken from 1ruv.pdb (*16*). (B) As in (A) but with 5′-CMP (in blue) bound. The coordinates for this diagram were taken from 1rnn.pdb.

nonproductive binding of cytidine. The latter assumption is based on observations made in high-resolution structures of RNase A (*16*). The side chain of Asp-83 in the RNase A−uridine vanadate and RNase S−UpcA complexes points toward the B1 subsite and is close to, but not hydrogen bonded to, $^{\gamma}$O of Thr-45 (cf. Figure 5A). However, in all structures with a cytidine bound in the B1 subsite (i.e., 1rnm.pdb, 1rnn.pdb, and 1rob.pdb), Asp-83 has turned away from Thr-45 in the B1 pocket (distance between Thr-45 $^{\gamma}$O and Asp-83 OD > 4 Å; Figure 5B) and interacts directly (1rob.pdb), or via water molecules (1rnm.pdb and 1rnn.pdb), with Arg-85. The side chain of Arg-101 of RNase 4 may help to fix Asp-80 in its orientation toward the B1 subsite by hydrogen bonding to its OD1 (Figure 3A). It, in turn, is kept in place by interacting with the α-carboxylate (Figure 3A).

Also, the side chain of Phe-42 of RNase 4 may be involved in fixing the position of Asp-80. In the model of free RNase 4, obtained using SWISSMODEL (*25*), the side chain of Phe-42 occupies the pyrimidine binding site through interaction with Phe-117 and has to move away upon substrate binding. This agrees with the observation that not only k_{cat}/K_m for CpA increases in RNase 4;F42V but also that for UpA is slightly larger than in the wild-type enzyme (*10*). The removal of the side chain of Phe-42 from the B1 subsite would move it between Arg-82 and Asp-80 (the residue corresponding to Asp-83 in RNase A). This would sterically hinder Asp-80 to move into an alternative position. Thus, in this model the improving effect on CpA catalysis of the RNase 4 mutation R101N, F42V, or T44A (Table 3 and ref *10*) would be caused by an increased freedom of Asp-80 to move upon binding of cytidine in the B1 subsite. The reduced catalysis with UpA would be due to the loss of, or decrease in, the hydrogen bond accepting properties of Thr-44.

The exact mechanism by which the close proximity of Asp-80 to Thr-44 and the B1 subsite to suppress CpA catalysis remains unclear. This question can probably only be addressed when the three-dimensional structure of RNase 4 in complex with uridine and cytidine analogues becomes available.

ACKNOWLEDGMENT

The authors thank Renate Matthies for the sequencing, Daniel Hess, FMI, and Werner Zürcher, Novartis AG, Basel, for the mass spectrometry, and Peter Müller and Franz Fischer for synthesizing oligonucleotides and peptides. The critical reading of the manuscript by Joachim Krieg, Andreas Löffler, and Wolfgang Gläsner is gratefully acknowledged.

REFERENCES

1. Zhou, H.-M., and Strydom, D. J. (1993) *Eur. J. Biochem. 217*, 401−410.
2. Beintema, J. J. (1987) *Life Chem. Rep. 4*, 333−389.
3. Beintema, J. J., Schüller, C., Irie, M., and Carsana, A. (1988) *Prog. Biophys. Mol. Biol. 51*, 165−192.
4. Richards, F. M., and Wyckoff, H. W. (1971) in *The Enzymes* (Boyer, P. D., Ed.) pp 647−806, Academic Press, New York.

5. Blackburn, P., and Moore, S. (1982) in *The Enzymes* (Boyer, P., Ed.) Vol. 15, pp 317−433, Academic Press, New York.
6. delCardayre, S. B., and Raines, R. T. (1994) *Biochemistry 33*, 6031−6037.
7. Mosimann, S. C., Newton, D. L., Youle, R. J., and James, M. N. G. (1996) *J. Mol. Biol. 260*, 540−552.
8. Acharya, K. R., Shapiro, R., Allen, S. C., Riordan, J. F., and Vallee, B. L. (1994) *Proc. Natl. Acad. Sci. U.S.A. 91*, 2915−2919.
9. Curran, T., Shapiro, R., and Riordan, J. F. (1993) *Biochemistry 32*, 2307−2313.
10. Vicentini, A. M., Kote-Jarai, Z., and Hofsteenge, J. (1996) *Biochemistry 35*, 9128−9132.
11. Shapiro, R., and Vallee, B. L. (1991) *Biochemistry 30*, 2246−2255.
12. Harper, J. W., and Vallee, B. L. (1989) *Biochemistry 28*, 1875−1884.
13. Shapiro, R., Fett, J. W., Strydom, D. J., and Vallee, B. L. (1986) *Biochemistry 25*, 7255−7264.
14. Vicentini, A., Hemmings, B. A., and Hofsteenge, J. (1994) *Protein Sci. 3*, 459−466.
15. delCardayre, S. B., and Raines, R. T. (1995) *J. Mol. Biol. 252*, 328−336.
16. Gilliland, G. L., Dill, J., Pechik, I., Svensson, L. A., and Sjölin, L. (1994) *Protein Pept. Lett. 1*, 60−65.
17. Hofsteenge, J., Servis, C., and Stone, S. R. (1991) *J. Biol. Chem. 266*, 24198−24204.
18. Knecht, R., and Chang, J.-Y. (1986) *Anal. Chem. 58*, 2375−2379.
19. Chang, J.-Y. (1984) *J. Chromatogr. 295*, 193−200.
20. Harper, J. W., Auld, D. S., Riordan, J. F., and Vallee, B. L. (1988) *Biochemistry 27*, 219−226.
21. Teschner, W., and Rudolph, R. (1989) *Biochem. J. 260*, 583−587.
22. Ho, S. N., Hunt, H. D., Horton, R. M., Pullen, J. K., and Pease, L. R. (1989) *Gene 77*, 51−59.
23. Sanger, F., Nicklen, S., and Coulson, A. R. (1977) *Proc. Natl. Acad. Sci. U.S.A. 74*, 5463−5467.
24. Vicentini, A. M., Kieffer, B., Matthies, R., Meyhack, B., Hemmings, B. A., Stone, S. R., and Hofsteenge, J. (1990) *Biochemistry 29*, 8827−8834.
25. Peitsch, M. C. (1996) *Biochem. Soc. Trans. 24*, 274−279.
26. Wlodawer, A., Miller, M., and Sjölin, L. (1983) *Proc. Natl. Acad. Sci. U.S.A. 80*, 3628−3631.
27. Bruenger, A., Brooks, C., III, and Karplus, M. (1985) *Proc. Natl. Acad. Sci. U.S.A. 82*, 8458−8462.
28. Hodges, R. S., and Merrifield, R. B. (1975) *J. Biol. Chem. 250*, 1231−1241.
29. Borkakoti, N., Palmer, R. A., Haneef, I., and Moss, D. S. (1983) *J. Mol. Biol. 169*, 743−755.
30. deMel, V. S. J., Martin, P. D., Doscher, M. S., and Edwards, B. F. P. (1992) *J. Biol. Chem. 267*, 247−256.

BI9803832